HHS Public Access

Author manuscript

Oncogene. Author manuscript; available in PMC 2022 June 01.

Published in final edited form as:

Oncogene. 2021 April ; 40(15): 2682–2696. doi:10.1038/s41388-021-01721-9.

EGFRvIII Tumorigenicity Requires PDGFRA Co-Signaling and Reveals Therapeutic Vulnerabilities in Glioblastoma

Alan T. Yeo[1,2], **Hyun Jung Jun**[1], **Vicky A. Appleman**[1], **Piyan Zhang**[1], **Hemant Varma**[3], **Jann N. Sarkaria**[4], **Al Charest**[1,5,*]

[1]Department of Medicine, Beth Israel Deaconess Medical Center, Harvard Medical School, Boston, MA, 02215, USA.

[2]Sackler School of Graduate Studies, Tufts University School of Medicine, Boston, MA, 02111, USA.

[3]Department of Pathology, Beth Israel Deaconess Medical Center, Harvard Medical School, Boston, MA, 02215, USA.

[4]Department of Radiation Oncology, Mayo Clinic, Rochester, MN, 55902, USA.

[5]Cancer Research Institute, Beth Israel Deaconess Medical Center, Boston, MA, 02215, USA.

Abstract

Focal amplification of epidermal growth factor receptor (EGFR) and its ligand-independent, constitutively active EGFRvIII mutant form are prominent oncogenic drivers in Glioblastoma (GBM). The EGFRvIII gene rearrangement is considered to be an initiating event in the etiology of GBM, however, the mechanistic details of how EGFRvIII drives cellular transformation and tumor maintenance remain unclear. Here, we report that EGFRvIII demonstrates a reliance on PDGFRA co-stimulatory signaling during the tumorigenic process in a genetically engineered autochthonous GBM model. This dependency exposes liabilities that were leveraged using kinase inhibitors treatments in EGFRvIII-expressing GBM patient-derived xenografts (PDXs), where simultaneous pharmacological inhibition of EGFRvIII and PDGFRA kinase activities is necessary for anti-tumor efficacy. Our work establishes that EGFRvIII-positive tumors have unexplored vulnerabilities to targeted agents concomitant to the EGFR kinase inhibitor repertoire.

Introduction

Glioblastoma (GBM) is a malignant primary brain cancer with a median survival of 14 months. The genomic landscape of GBM is well characterized (1–3) and aberrant overexpression of EGFR is the most commonly observed genomic event in GBM, occurring in ~65% of all GBM patients (1–3). Along with EGFR copy number variants, deletion and mutations of the INK4a/ARF (Cdkna) locus occurs in >90% of EGFR positive cases and deletion and/or mutations of PTEN (~41%) are also frequently observed. Focally amplified

[*]**Corresponding Author:** Alain Charest, Cancer Research Institute, Beth Israel Deaconess Medical Center, Department of Medicine, Harvard Medical School, 330 Brookline Ave, Boston, MA, 02215. acharest@bidmc.harvard.edu, 617-667-5687.

Competing interests: The authors declare that they have no competing interests.

EGFR has been recently shown to reside on extrachromosomal DNA (ecDNA) (4–7). In half of the EGFR-amplified tumors (representing ~30% of all GBM patients), an intragenic in-frame deletion of exons 2 to 7 of Egfr results in a transcript that codes for a constitutively activated, ligand-independent receptor known as EGFRvIII.

Opinions on the role of EGFRvIII in gliomagenesis are contradictory. Early reports suggested that EGFRvIII positivity conferred a worse survival on patients (8, 9), however this observation was not sustained in more recent analyses of larger cohorts (10–12). Studies on paired EGFRvIII positive primary and recurrent GBMs revealed that in most cases (~80%), EGFRvIII rearrangement is qualitatively retained in recurrent tumors (12, 13). However, the levels of EGFRvIII transcripts are significantly reduced or undetectable in ~50% of recurrent GBMs (12–14), seemingly suggesting that EGFRvIII expression is influenced epigenetically, perhaps as a result of fractionated radiation and temozolomide treatments. Remarkably, there are few cases in which EGFRvIII expression is detected only in recurrent GBM tumors (12, 13). More recently, in-depth analyses at the single cell level revealed that GBM heterogeneity derives from significant clonal evolutions during gliomagenesis (15–18), and perhaps the emergence and attenuation of EGFRvIII-positive cells is a manifestation of the dynamic clonal changes of GBMs. EGFRvIII expression is heterogeneous, sometimes detected in only a small percentage of tumor cells (19, 20), which undermines the rationale for EGFRvIII-targeted therapies. Although the significance of EGFRvIII expression in clinical samples is debatable, *ex-vivo* studies on models of ectopic expression of EGFRvIII in GBM cell lines unequivocally demonstrate that EGFRvIII-positive cells are more resistant to apoptosis, more invasive, display greater proliferation rates and angiogenesis and enhanced ability to form xenograft tumors when compared to their parental counterparts (reviewed in (21, 22)). On the surface, these observations would suggest that EGFRvIII positivity confers accrued malignancy to GBMs. However, the difficulty in reconciling clinical and laboratory observations demonstrate a need for further investigations into EGFRvIII bona fide role in gliomagenesis in clinically and genetically relevant model systems.

Members of the EGFR family are known to homo- and heterodimerize (23). Structural studies of EGFR have produced models of homodimerization and shaped our insights into the mechanisms of kinase activation. The structural details of intra-family heterodimerization however remain ill defined in comparison. The consensus of many analyses is that EGFRvIII is capable of forming both homo- and heterodimers with EGFR WT (24–31), while the ability of EGFRvIII to heterodimerize with other members of the EGFR family remains to be addressed. Abundant evidence support the notion that EGFR WT can physically interact with and/or modulate the activities of many other receptor tyrosine kinases (RTKs) including AXL, EphA2, FGFR1, FGFR3, IGF-1R, HGFR/MET, PDGFRA, PDGFRB, Ron, ROR1, STYK1, TrkA, and TrkB in various tissues and cancers (recently reviewed in (32)). Similarly, studies have shown that EGFRvIII can also dimerize with monomers of other receptor tyrosine kinases such as the hepatocyte growth factor receptor (HGFR) and platelet-derived growth factor receptor A (PDGFRA) (33–35) and directly influence their function.

In addition to EGFR, amplification, over-expression, and mutations of PDGFRA is the second most common genetic aberrations of receptor tyrosine kinases in GBM occurring in 13.1% of patients (1). PDGF ligands induce homo- and heterotypic dimerization and activation of PDGFRA and PDGFRB to elicit various intracellular signaling pathways and physiological responses (36). De-regulation of PDGF–PDGFR signaling axis leads to a number of cancers, including GBMs (37). We recently reported on a comprehensive review of the signaling pathways downstream of activated PDGFRs (38) and observed a significant overlap between the signaling events downstream of activated PDGFRA and EGFR (38).

The prevalence of EGFR-activating genomic events in gliomas, lung adenocarcinomas and other cancers has stimulated the development of targeted small molecule inhibitors that differ in their modes of action. Fueled by structural mechanistic insights, reversible and covalent/irreversible inhibitors of EGFR have been developed, which bind the kinase domain and inhibit its kinase activity while the receptor is in either an active (Type I inhibitors) or inactive (Type II inhibitors) conformation (recently reviewed in (39)). With these structural details in mind, the following first and second generation EGFR inhibitors were developed: Gefitinib (reversible Type I), Canertinib (irreversible Type I), Lapatinib (reversible Type II) and Neratinib (irreversible Type II). Efficacy of kinase inhibition and anticancer effects for these inhibitors have been studied extensively in the context of EGFR WT and EGFR kinase domain mutants in lung cancers but not against EGFRvIII-positive GBMs. Although clinically very successful in lung cancers, substantial therapeutic advances aimed at inhibiting EGFR in GBM remain unrealized (40). These clinical failures in GBM are partly due to the emergence of compensatory mechanisms or a non-dependency on EGFR for survival (40). We surmised that a better understanding of EGFRvIII biology during GBM initiation and maintenance is needed. Using a combination of GBM patient-derived xenografts (PDXs) and genetically engineered mouse models, we demonstrate an obligatory requirement on additional signaling for EGFRvIII-driven gliomagenesis, which sets up a dependency on co-signaling that can be exploited pharmacologically.

Results

EGFRvIII positive GBM PDX cells are sensitive to Canertinib.

We determined the effects of type I and type II, reversible and irreversible EGFR inhibitors on EGFRvIII-positive GBM PDX cell cultures (41–43). Treatment of cells from four GBM PDXs with comparable EGFRvIII expression levels (Fig. S1A) and two low background level EGFR expressing and non-activated control GBM PDX cultures with 1 or 10 μM of Gefitinib (reversible Type I), Canertinib (irreversible Type I), Lapatinib (reversible Type II) and Neratinib (irreversible Type II) led to similar levels of EGFR kinase activity inhibition (up to >90%) as measured by the levels of EGFR autophosphorylation at Y1068 in cells from EGFRvIII-positive PDXs but not in the controls (Fig. 1A, Fig. S1B). Surprisingly, cell viability measured after 24 hr treatments revealed that only Canertinib (10 μM) treatment resulted in a consistent reduction in viability in the EGFRvIII positive PDX cells (Fig. 1B). EGFR negative PDX control cells were not affected (Fig. 1B). To better understand the effects of Canertinib on GBM cell growth, we selected GBM6, GBM39 and GBM59 for more detailed analysis. The viability of EGFRvIII-positive GBM6, GBM39 and GBM59

PDX cells was rapidly decreased to 50% viability within 10–15 hr (Fig. 1C). Consistent with these observations are the increases in AnnexinV positive cells (Fig. 1D) indicating the initiation of an apoptotic response upon treatment. These results demonstrated that inhibition of EGFR kinase activity alone is not sufficient to trigger apoptotic responses in human EGFRvIII positive PDXs and that Canertinib can induces a rapid (within 24 hr) apoptotic cell death response.

A longitudinal analysis of the activation of the canonical EGFR signaling pathways MEK1/2-ERK1/2 and PI3K-AKT in the context of Gefitinib and Canertinib treatments in GBM6 and GBM59 revealed that EGFR kinase activity, as measured by the levels of phospho-EGFR Y1068 is rapidly inhibited by both Gefitinib and Canertinib (Fig. 1E, Fig. S1C). Levels of phospho-ERK1/2, a surrogate of MEK1/2 kinase activity, initially declined upon treatments with both inhibitors but remarkably, rebounded in the Gefitinib treated cells back to baseline levels and above after 1.5 hours of treatment whereas in Canertinib treated cells, the levels of phospho-ERK1/2 remained low throughout the experimental time frame of 8 hr (Fig. 1E, Fig. S1C). In contrast, levels of phospho-AKT, a surrogate of PI3K activity, were diminished within an hour of Gefitinib and Canertinib treatments and remained low throughout in Canertinib treated cells and slightly increased in Gefitinib treated cells (Fig. 1E, Fig. S1C, D). At the 8 hr time point, the levels of phospho-ERK1/2 and phospho-AKT in Gefitinib treated cells were significantly higher than in Canertinib treated cells. Analysis of cleaved PARP levels over time during treatment demonstrated an accumulation of apoptotic cells over time in the Canertinib treatment, consistent with the prior AnnexinV observation that Canertinib treatment induces apoptosis more significantly than Gefitinib treatment (Fig. 1E, Fig. S1C, D).

We also observed the anti-growth effects of Canertinib *in vivo*. Daily treatment of GBM6 PDX tumor-bearing mice with Gefitinib (100 mg/kg p.o.) did not affect the growth of GBM6 tumors when compared to vehicle (Fig. 2A) however, treatment with Canertinib (100 mg/kg p.o.) led to a significant reduction in tumor growth even though the levels of phospho-EGFR were similarly reduced in Gefitinib and Canertinib treated tumors (Fig. 2B–C). Moreover, levels of phospho-AKT and phospho-ERK1/2 were both reduced in Canertinib treated tumors compared to Gefitinib treated tumors (Fig. 2B). Together, these results indicate that treatment of EGFRvIII-positive GBM PDXs using Canertinib but not Gefitinib leads to reduction of cell viability, attenuation of MEK-ERK and PI3K signaling, increase in apoptosis and decrease in tumor growth *in vivo*.

Canertinib treatments elicit reductions in PDGFRA and EGFRvIII kinase activities

Kinase inhibitors notoriously display varied selectivity towards kinases (44) that often result in multi-targets inhibition when used at high concentrations. The noticeable differences in signaling, cellular growth and anti-tumor efficacies *in vitro* between low (1 μM) and high (10 μM) doses of Canertinib suggest that other kinases in addition to EGFRvIII are inhibited. To determine if high concentrations of Canertinib inhibit other RTKs in our GBM PDXs, we performed a 49 tyrosine kinase phospho-RTK array screen by comparing GBM6 PDX cells treated with vehicle control, 10 μM Gefitinib, 1 μM Canertinib or 10 μM Canertinib (Fig. 3A). We observed that 10 μM Canertinib resulted in a 93% reduction

of PDGFRA phosphorylation whereas 10 μM Gefitinib and 1 μM Canertinib resulted in a lesser reduction of PDGFRA phosphorylation (65% and 72% respectively) (Fig. 3A). This observation was confirmed by western blots of GBM6 PDX cells treated with vehicle, Gefitinib (10 μM) or Canertinib (1 and 10 μM) that measured the levels of phospho-EGFR and phospho-PDGFRA (Fig. 3B, Fig. S2A). The levels of PDGFRA in GBM6, GBM39 and GBM59 are similar (Figure S2B) and significant reduction of phosphorylated PDGFRA is only observed in cells treated with 10 μM Canertinib and not in those treated with 1 μM and 10 μM Gefinitib, Lapatinib or Neratinib in GBM6, GBM39 and GBM59 (Fig. 3C, Fig. S2C).

The anti-tumor effects of Canertinib *in vivo* are dose dependent (Fig. 3D). As observed earlier, Gefitinib treatment (100 mg/kg q.d.p.o) had no effect on tumor growth even though it significantly reduced (96.1 ±4.6%) the levels of EGFR autophosphorylation in tumors (Fig. 3E, Fig. S2C). In contrast, low dose (10 mg/kg q.d. p.o.) of Canertinib resulted in a tumor static effect and was associated with a 95.9% ±4.8% reduction in EGFR autophosphorylation (Fig. 3E, Fig. S2C). Higher doses of Canertinib (50, 100, 250 mg/kg q.d. p.o.) led to reduction in tumor sizes, which correlated with maximal levels of EGFR kinase inhibition (>99%) (Fig. 3E, Fig. S2C). The levels of phospho-PDGFRA were marginally reduced by treatment of Gefitinib (13.4% ±2.7%) and were decreased in a dose-dependent manner with increasing Canertinib dosing reaching a 78.3% ±2.3% reduction in the 250 mg/kg q.d.p.o) treatment (Fig. 3E, Fig. S2C). Immunohistochemistry analysis of FFPE sections of the control and Gefitinib- and Canertinib-treated GBM6 tissues showed that the antitumor growth effects observed with Canertinib correlated with decreases in the proliferative marker Ki-67 (MIB-1) and increases in the apoptotic marker cleaved caspase 3 (CC3) (Fig. 3F).

Simultaneous attenuation of MEK and PI3K signaling triggers apoptosis in GBM PDX cells.

The sustained inhibition of both MEK and PI3K activity observed in Canertinib treated cells parallels their apoptotic response (Fig. 1E), whereas Gefitinib treatment did not elicit a sustained inhibition of MEK nor apoptosis. Therefore, in the context of PI3K inhibition, continuous MEK inhibition appears to be necessary for initiating an apoptotic response in GBM6 and GBM59 cells. Since both EGFR and PDGFRA signal through PI3K–AKT and MEK-ERK pathways, we substantiated our previous observation by treating GBM6 PDX cells with the MEK1/2 inhibitor tool compound PD0325901 and the PI3K inhibitor GDC-0941 (Pictilisib) (45, 46) individually and in combination. We observed that combined inhibition of PI3K and MEK1/2 led to sustained apoptosis by cleavage of PARP in a time dependent manner and to levels similar to those seen during treatment with 10 μM of Canertinib, whereas treatment with Pictilisib or PD0325901 alone did not (Fig. 4A, Fig. S3A).

Previous observations demonstrated a physical interaction between EGFR and PDGFRA in GBM (33). Here, we established a functional interaction between EGFR and PDGFRA. Co-treatment with the PDGFRA inhibitor Ponatinib (AP24534 (47)) and Gefitinib for 24 hr is sufficient to induce apoptosis, confirming the co-dependency of both EGFRvIII and PDGFRA signaling (Fig. 4B, Fig. S3B). Time course experiments revealed that either 10 μM Gefitinib or 1 μM Canertinib in combination with the PDGFRA inhibitor Axitinib

(AG-013736 (47)), can simultaneously suppress PI3K-AKT and MEK-ERK pathways, in a manner similar to 10 μM Canertinib (Fig. 5A, Fig. S4A), suggesting that EGFRvIII and PDGFRA converge on these two major signaling pathways in GBM6. Together, these results indicate that simultaneous suppression of PI3K/AKT and MEK/ERK signaling pathways downstream of EGFR and PDGFRA in EGFRvIII positive GBM PDX cells elicits an apoptotic response.

Inhibition of PDGFRA sensitizes GBM PDX cells to EGFR inhibition.

We further substantiated the reliance of PDGFRA activity for EGFR inhibition sensitivity with an additional pharmacological inhibitor of PDGFR. Time course treatments with either 10 μM Gefitinib or 1 μM Canertinib in combination with the PDGFRA inhibitor Axitinib (AG-013736 (47)), simultaneously suppressed PI3K-AKT and MEK-ERK pathways, in a manner similar to 10 μM Canertinib (Fig. 5A, Fig. S4A), further suggesting that EGFRvIII and PDGFRA converge on these two major signaling pathways in GBM6.

Similarly, the apoptotic response triggered by dual inhibition of EGFRvIII and PDGFRA was further confirmed using annexinV staining by flow cytometry in GBM6 and GBM39 (Fig. 5B). To validate these results, we performed genetic disruption of PDGFRA with siRNAs in GBM6 and GBM39 (Figure 5C–E, Figure S4B). We determined that all three siRNAs produced significant knock down of PDGFRA as measured by PDGFRA western blotting (Figure 5C). The substantial reduction of PDGFRA protein expression observed did not disrupt the ability of Gefitinib and Canertinib to inhibit EGFR (Figure 5D) and conferred apoptotic responses to EGFR inhibition with 10 μM Gefitinib or 1 μM Canertinib (Fig. 5E). Together, these results indicate that single receptor inhibition is not sufficient to attenuate the levels of PI3K/AKT and MEK/ERK signaling but rather that an elimination of PDGFRA expression (or inhibition of activity) in EGFRvIII positive GBM6 and GBM39 PDX cells renders the cells sensitive to EGFR inhibition.

Ontogenesis of EGFRvIII dependence on co-stimulatory signaling

Experimental evidence demonstrates that EGFRvIII can dimerize with monomers of hepatocyte growth factor receptor (HGFR, cMET) or PDGFRA (33, 34). This suggests that a dependence on co-signaling events for EGFRvIII function is necessary for gliomagenesis. We surmised that EGFRvIII's necessity for additional signal for tumor maintenance might result from early events during tumor initiation, which would set the stage for dependencies on co-signaling inputs for tumor maintenance. To experimentally ascertain this, we leveraged our conditional, genetically engineered lox-stop-lox EGFRvIII;Cdkn2a$^{-/-}$;PTEN$^{lox/lox}$ -driven mouse model (48). In this model, intracranial ectopic expression of adenovirus Cre (AdCre) in adult animals removes a floxed transcriptional-translational stop cassette that is located upstream of a human EGFRvIII cDNA resulting in clinically relevant levels of EGFRvIII expression and concomitant loss of PTEN expression (48). In the context of Cdkn2a and PTEN loss, EGFRvIII drives the formation of fully penetrant GBMs with short latencies (48) (Fig. 6A). Surprisingly, ectopic expression of EGFRvIII together with loss of Cdkn2a does not lead to GBM formation (Fig. 6A), suggesting that additional signaling events brought about by the loss of PTEN are necessary for EGFRvIII to drive tumorigenesis *in vivo*.

To better understand the signaling events behind this dependency, we expressed EGFRvIII in Cdkn2a$^{-/-}$;PTEN$^{lox/lox}$ primary mouse astrocytes and performed *in vitro* transformation assays and signaling analyses in the context of normal PTEN expression and loss of PTEN. Note that these cells are expressing normal levels of PTEN and can be rendered PTEN null by infection with AdCre, thus creating PTEN null syngeneic cells (Fig. S5). Using growth in soft agar as a measure of cellular transformation, parental Cdkn2a$^{-/-}$ astrocytes, Cdkn2a$^{-/-}$;PTEN$^{lox/lox}$ astrocytes and EGFRvIII;Cdkn2a$^{-/-}$;PTEN$^{lox/lox}$ astrocytes (wild type levels of PTEN expression) failed to grow in non-adherent semi-solid medium conditions (Fig. 6B). We observed that loss of PTEN (AdCre infected syngeneic cells) in these cells led to an increase in the number of cells growing in soft agar (Fig. 6B). Mechanistically, expression of EGFRvIII in Cdkn2a$^{-/-}$;PTEN$^{lox/lox}$ astrocytes (wild type levels of PTEN expression) result in modest increases in activation of canonical signaling events downstream of EGFR, that is MEK-ERK and to a lesser extend PI3K-AKT (Fig. 6C). Loss of PTEN however, resulted in a significant increase in the levels of phospho-EGFR, MEK-ERK and PI3K-AKT signaling (Fig. 6C). Together, these results support the notion that EGFRvIII expression alone is insufficient to transform mouse astrocytes and requires additional and simultaneous MEK-ERK and PI3K-AKT activation to reach a threshold of signaling strength to achieve cellular transformation.

PDGFRA activity is necessary for EGFRvIII-driven GBM formation in mice

To support our observations of EGFRvIII conditional oncogenecity and to further validate the functional interaction between EGFRvIII and PDGFRA, we leveraged our LSL-EGFRvIII;Cdkn2a$^{-/-}$ genetically engineered mice to activate PDGFRA in the context of EGFRvIII signaling. Here we performed intracranial injection of a lentivirus co-expressing a tetracycline-inducible PDGFA cDNA and a constitutive Cre recombinase (Fig. 7A). Infected cells produce Cre, which triggers the expression of EGFRvIII and doxycycline (DOX) administration results in PDGF-A expression and consequently, PDGFRA activation. Control and DOX-treated mouse cohorts were established and monitored for survival. EGFRvIII;Cdkn2a$^{-/-}$ mice expressing PDGFA (+DOX) readily formed lethal tumors whereas EGFRvIII;Cdkn2a$^{-/-}$ or PDGFA (+DOX) Cdkn2a$^{-/-}$ controls did not (Fig. 7B). Histopathological analysis of the PDGFA-EGFRvIII;Cdkn2a$^{-/-}$ tumors was performed (Fig. 7C, i). Tumors, which were centrally located surrounding the area of virus injection, displayed dense cellularity with areas of pseudopalisading necrosis and microvascular proliferation (Fig. 7C, ii). Neoplastic cells had moderate nuclear atypia and showed frequent mitoses (Fig. 7C, iii). Immunohistochemical staining for the astrocytic marker glial fibrillary acidic protein (GFAP) showed positive staining in a subset of tumor cells and also highlighted their glial processes, whereas staining for the neuronal marker NeuN was negative in tumor cells (Fig. 7C, iv & v, respectively), confirming the glial lineage of these tumors. Staining for human EGFR showed ubiquitous expression in tumor cells and allowed detection of highly invasive tumor cells, infiltrating normal brain parenchyma (Fig. 7C, vi). Overall, these histological features that are characteristic of patient GBMs revealed that PDGFRA activity contributed to EGFRvIII-driven GBM tumorigenesis.

To solidify our previous observations and to gain further mechanistic insights into the functional interaction between EGFRvIII and PDGFRA, we isolated primary cultures from

the PDGFA-EGFRvIII;Cdkn2a−/− GBMs above. Consistent with our previous observations in EGFRvIII positive GBM PDXs, *ex vivo* cultures of these PDGFA-EGFRvIII;Cdkn2a$^{-/-}$ GBM tumor cell lines displayed similar sensitivity to high dose (10 μM) of Canertinib, whereas all other EGFR TKIs tested failed to stimulate apoptosis (Fig. 7D). In addition, the observed apoptosis that is induced with 10 μM Canertinib parallels with suppression of MEK-ERK and PI3K-AKT signaling pathways (Fig. 7E). Finally, pharmacological suppression of MEK and PI3K pathways with inhibitors also triggered an apoptotic response in these cells (Fig. 7E). Together, these results further support our observations that EGFRvIII necessitates additional signaling, here in the form of PDGFRA signaling, for gliomagenesis.

Discussion

EGFR and EGFRvIII are important oncogenic drivers of GBM. The structural details of EGFRvIII activation remain unknown, hindering our knowledge of the molecular mechanisms of kinase inhibitor actions for this mutant receptor. Here we used a combination of GBM PDXs that are positive for EGFRvIII expression and genetically engineered mouse models of EGFRvIII-driven glioma to explore the mechanisms of how EGFRvIII transforms cells and how the ensuing signaling pathways wire cells to be sensitive or resistant to different classes of EGFR inhibitors.

Our models reveal important aspects of EGFRvIII-driven gliomagenesis that were previously unknown. First, potent (>90%) inhibition of EGFRvIII kinase activity, achieved with all classes of EGFR inhibitors, had no effect on cell growth of GBM PDXs except for when treated with high concentrations of Canertinib. Our results reinforce previous observations that GBMs are not oncogenically addicted to EGFR (49), which may explain the numerous failures of EGFR TKIs in clinical settings (40). High concentrations of Canertinib did not result in additional kinase inhibition but instead led to a simultaneous attenuation of MEK-ERK and PI3K pathway signaling and apoptosis in EGFRvIII-positive GBMs. These observations were further refined using concomitant MEK and PI3K inhibitor treatments. The dynamics of inactivation of MEK-ERK and PI3K-AKT signaling under EGFR inhibitor treatments are revealing. Gefitinib and Canertinib treatments lead to immediate MEK-ERK and PI3K-AKT inactivation, however only Gefitinib treated cultures showed levels of pERK and pAKT rebound over time whereas Canertinib treated cultures showed a significantly reduced MEK-ERK and PI3K-AKT signaling. This raises the possibility that the dominant driver in these cells is EGFRvIII and upon its inhibition with Gefitinib, a lag period exist before signaling from PDGFRA ensues, thus embodying the transient nature of MEK-ERK and PI3K-AKT inhibition.

Simultaneous inhibition of MEK-ERK and PI3K has proven to be efficacious in a mouse model of KRasG12D-driven GBM (50). Unfortunately, clinical evidence in non-GBM patients demonstrated that this combination may be limited due to synergistic toxicity (51–55). Our results support an alternative approach, which is to inhibit these pathways using inhibitors of upstream drivers, such as simultaneous inhibition of PDGFRA and EGFRvIII to concomitantly shut down both MEK-ERK and PI3K. This might provide a more efficient and safer window than combination of MEK and PI3K inhibitors.

Second, EGFRvIII oncogenicity is context dependent. When expressed at physiological levels (48) in the context of deleted Cdkn2a, EGFRvIII is incapable of driving astrocyte transformation *in vitro* and *in vivo*. This is in contrast to previous work on the transformation capacity of EGFRvIII in Cdkn2a null mouse astrocytes (56), perhaps reflecting a difference in the levels of EGFRvIII expression in the two systems. We showed that EGFRvIII-driven transformation and tumorigenesis rely on additional signaling events, either in the form of loss of PTEN or activation of PDGFRA. In the context of loss of PTEN, enhanced PI3K signaling is observed and interestingly, MEK-ERK signaling as well. Similarly, PTEN loss-mediated cross activations of the MAPK pathway have been reported in human and mouse cancer models (57–62), but never in GBM. In our system, we discovered that loss of PTEN resulted in a significant increase in the levels of phospho-EGFRvIII and simultaneous activation of MEK-ERK and PI3K. These observations require further mechanistic investigations.

Third, activation of PDGFRA is another mechanism that EGFRvIII can use for gliomagenesis. We surmised that this dependency consequently wires cells with redundancy in signaling once tumors are formed, such that single target inhibition is now ineffective. The functional interaction between EGFRvIII and PDGFRA is supported by evidence of co-expression in GBMs (33, 35, 63) and physical dimerization between EGFR and PDGFRA (33). In fact, EGFR has been reported to dimerize with numerous RTKs (reviewed in (32)). However, the structural details of EGFR heterodimerization to other RTKs are completely unknown and future insights remain hindered by many technical challenges.

Taken together, our results suggest a co-dependency of PDGFRA signaling in EGFRvIII positive GBM PDXs that converge on both downstream PI3K-AKT and MEK-ERK signaling. Moreover, high concentrations of Canertinib, which concurrently target these pathways, can be leveraged as a method of inducing apoptosis in these GBM cells. It is currently unclear how EGFRvIII and PDGFRA contribute to the action of PI3K-AKT and MEK-ERK signaling, as our results from single agent control treatments show only modest inhibition of both pAKT and pERK, not preference for only pAKT or pERK. These results reflect the complexity and plasticity of RTK interactions and warrant future investigations to better understand the complexity of RTK networks. Finally, by understanding signaling requirements in the process of cellular transformation and signaling wiring, one may be able to take advantage of unrecognized dependencies with clinical implications

Materials and Methods

PDGF-A-EGFRvIII Conditional Mice.

All mouse procedures were performed in accordance with Beth Israel Deaconess Medical Center recommendations for the care and use of animals, and were maintained and handled under protocols approved by the Institutional Animal Care and Use Committee. The conditional EGFRvIII genetically engineered mouse strain has been described in detail elsewhere (48). Briefly, a CAG-floxed stop cassette EGFRvIII cDNA minigene was targeted into the mouse collagen1α1 gene locus and crossed to constitutive Cdkn2a null mice (64) and conditional PTEN mice (65). Initiation of EGFRvIII expression in the CNS was accomplished by stereotactic intracranial injections of a PDGF-A-Cre lentivirus.

Stereotactic injections, generation of primary cultures are described in greater detail in the Supplementary Materials and Methods section.

Virus Construct Design, Production and Titer Determination.

The pSLIK (single lentivector for inducible knock-down) vector system (66) was modified to express the human PDGF-A cDNA and Cre recombinase as described elsewhere (37). Briefly, the modification of the original lentiviral vector platform supports constitutive expression of a Tet-transactivating component (rtTa3) under a Ubc promoter and the cDNA for Cre recombinase through an Internal Ribosomal Entry Site (IRES) and inducible PDGF-A expression under doxycycline (DOX) treatments. Viruses were produced by co-transfection of 293T cells with packaging vectors and purified by ultracentrifugation of conditioned media, resuspended in PBS, aliquoted in single use amounts and stored at −80^{o}C. To standardize intracranial injections with identical viral titers, viral preparations were functionally titered for Cre activity by serial dilution infection of immortalized fibroblasts derived from Cdkn2a-null conditional LSL-tdTomato Ai9 reporter mouse strain (67).

siRNA transfection

GBM6 cells were reverse transfected with single siRNAs targeting human PDGFRA obtained from Dharmacon (Horizon). Briefly, pre-trypsinized single cell suspensions were incubated with transfection mix containing Dharmacon transfection reagent 1 with single siPDGFRA in Opti-MEM reduced serum medium (Gibco) and plated at 10^5 cells per well in DMEM containing 10% FBS without antitiotic-antimycotics. The medium was replaced ~ 18 hours later with DMEM low serum media (0.1% FBS) for 24 h prior to inhibitor treatment. The target sequences of siPDGFRA are as follows:

siScrambled: UGGUUUACAUGUCGACUAA

siPDGFRA #1: GAAUAGGGAUAGCUUCCUG

siPDGFRA #2: GAGCUUCACCUAUCAAGUU

siPDGFRA #3: GACAGUGGCCAUUAUACUA

Statistical analysis.

Statistical analyses were carried out using GraphPad Prism 7. Two-tailed Student’s t-tests were used for single comparison. P-values of < 0.05 were considered statistically significant.

Supplementary Material

Refer to Web version on PubMed Central for supplementary material.

Acknowledgements.

The authors thank Drs. Shruti Rawal and Shibani Mukherjee for critical review of the manuscript. The authors also thank Patrick Hyland (Tufts University), Ilyse Blazar (Boston University), Derrek Schartz (Tufts University) for their technical assistance. This work was supported by NIH grants R01 CA229784 and R21 CA245337 to AC and by internal funding to the Mayo Clinic GBM PDX National Resource to J.N.S.

Funding:

This work was supported by NIH grants R01 CA229784 and R21 CA245337 to AC and by internal funding to the Mayo Clinic GBM PDX National Resource to J.N.S.

References

1. Brennan CW, Verhaak RG, McKenna A, Campos B, Noushmehr H, Salama SR, Zheng S, Chakravarty D, Sanborn JZ, Berman SH, Beroukhim R, Bernard B, Wu CJ, Genovese G, Shmulevich I, Barnholtz-Sloan J, Zou L, Vegesna R, Shukla SA, Ciriello G, Yung WK, Zhang W, Sougnez C, Mikkelsen T, Aldape K, Bigner DD, Van Meir EG, Prados M, Sloan A, Black KL, Eschbacher J, Finocchiaro G, Friedman W, Andrews DW, Guha A, Iacocca M, O'Neill BP, Foltz G, Myers J, Weisenberger DJ, Penny R, Kucherlapati R, Perou CM, Hayes DN, Gibbs R, Marra M, Mills GB, Lander E, Spellman P, Wilson R, Sander C, Weinstein J, Meyerson M, Gabriel S, Laird PW, Haussler D, Getz G, Chin L, Network TR, The somatic genomic landscape of glioblastoma. Cell 155, 462–477 (2013). [PubMed: 24120142]

2. McLendon R, Friedman A, Bigner D, Van Meir EG, Brat DJ, Mastrogianakis M, Olson JJ, Mikkelsen T, Lehman N, Aldape K, Alfred Yung WK, Bogler O, Vandenberg S, Berger M, Prados M, Muzny D, Morgan M, Scherer S, Sabo A, Nazareth L, Lewis L, Hall O, Zhu Y, Ren Y, Alvi O, Yao J, Hawes A, Jhangiani S, Fowler G, San Lucas A, Kovar C, Cree A, Dinh H, Santibanez J, Joshi V, Gonzalez-Garay ML, Miller CA, Milosavljevic A, Donehower L, Wheeler DA, Gibbs RA, Cibulskis K, Sougnez C, Fennell T, Mahan S, Wilkinson J, Ziaugra L, Onofrio R, Bloom T, Nicol R, Ardlie K, Baldwin J, Gabriel S, Lander ES, Ding L, Fulton RS, McLellan MD, Wallis J, Larson DE, Shi X, Abbott R, Fulton L, Chen K, Koboldt DC, Wendl MC, Meyer R, Tang Y, Lin L, Osborne JR, Dunford-Shore BH, Miner TL, Delehaunty K, Markovic C, Swift G, Courtney W, Pohl C, Abbott S, Hawkins A, Leong S, Haipek C, Schmidt H, Wiechert M, Vickery T, Scott S, Dooling DJ, Chinwalla A, Weinstock GM, Mardis ER, Wilson RK, Getz G, Winckler W, Verhaak RG, Lawrence MS, O'Kelly M, Robinson J, Alexe G, Beroukhim R, Carter S, Chiang D, Gould J, Gupta S, Korn J, Mermel C, Mesirov J, Monti S, Nguyen H, Parkin M, Reich M, Stransky N, Weir BA, Garraway L, Golub T, Meyerson M, Chin L, Protopopov A, Zhang J, Perna I, Aronson S, Sathiamoorthy N, Ren G, Wiedemeyer WR, Kim H, Won Kong S, Xiao Y, Kohane IS, Seidman J, Park PJ, Kucherlapati R, Laird PW, Cope L, Herman JG, Weisenberger DJ, Pan F, Van Den Berg D, Van Neste L, Mi Yi J, Schuebel KE, Baylin SB, Absher DM, Li JZ, Southwick A, Brady S, Aggarwal A, Chung T, Sherlock G, Brooks JD, Myers RM, Spellman PT, Purdom E, Jakkula LR, Lapuk AV, Marr H, Dorton S, Gi Choi Y, Han J, Ray A, Wang V, Durinck S, Robinson M, Wang NJ, Vranizan K, Peng V, Van Name E, Fontenay GV, Ngai J, Conboy JG, Parvin B, Feiler HS, Speed TP, Gray JW, Brennan C, Socci ND, Olshen A, Taylor BS, Lash A, Schultz N, Reva B, Antipin Y, Stukalov A, Gross B, Cerami E, Qing Wang W, Qin LX, Seshan VE, Villafania L, Cavatore M, Borsu L, Viale A, Gerald W, Sander C, Ladanyi M, Perou CM, Neil Hayes D, Topal MD, Hoadley KA, Qi Y, Balu S, Shi Y, Wu J, Penny R, Bittner M, Shelton T, Lenkiewicz E, Morris S, Beasley D, Sanders S, Kahn A, Sfeir R, Chen J, Nassau D, Feng L, Hickey E, Weinstein JN, Barker A, Gerhard DS, Vockley J, Compton C, Vaught J, Fielding P, Ferguson ML, Schaefer C, Madhavan S, Buetow KH, Collins F, Good P, Guyer M, Ozenberger B, Peterson J, Thomson E, Comprehensive genomic characterization defines human glioblastoma genes and core pathways. Nature, (2008).

3. Verhaak RG, Hoadley KA, Purdom E, Wang V, Qi Y, Wilkerson MD, Miller CR, Ding L, Golub T, Mesirov JP, Alexe G, Lawrence M, O'Kelly M, Tamayo P, Weir BA, Gabriel S, Winckler W, Gupta S, Jakkula L, Feiler HS, Hodgson JG, James CD, Sarkaria JN, Brennan C, Kahn A, Spellman PT, Wilson RK, Speed TP, Gray JW, Meyerson M, Getz G, Perou CM, Hayes DN, Integrated genomic analysis identifies clinically relevant subtypes of glioblastoma characterized by abnormalities in PDGFRA, IDH1, EGFR, and NF1. Cancer Cell 17, 98–110 (2010). [PubMed: 20129251]

4. Verhaak RGW, Bafna V, Mischel PS, Extrachromosomal oncogene amplification in tumour pathogenesis and evolution. Nat Rev Cancer 19, 283–288 (2019). [PubMed: 30872802]

5. deCarvalho AC, Kim H, Poisson LM, Winn ME, Mueller C, Cherba D, Koeman J, Seth S, Protopopov A, Felicella M, Zheng S, Multani A, Jiang Y, Zhang J, Nam DH, Petricoin EF, Chin L, Mikkelsen T, Verhaak RGW, Discordant inheritance of chromosomal and extrachromosomal DNA elements contributes to dynamic disease evolution in glioblastoma. Nat Genet 50, 708–717 (2018). [PubMed: 29686388]

6. Turner KM, Deshpande V, Beyter D, Koga T, Rusert J, Lee C, Li B, Arden K, Ren B, Nathanson DA, Kornblum HI, Taylor MD, Kaushal S, Cavenee WK, Wechsler-Reya R, Furnari FB, Vandenberg SR, Rao PN, Wahl GM, Bafna V, Mischel PS, Extrachromosomal oncogene amplification drives tumour evolution and genetic heterogeneity. Nature 543, 122–125 (2017). [PubMed: 28178237]
7. Nathanson DA, Gini B, Mottahedeh J, Visnyei K, Koga T, Gomez G, Eskin A, Hwang K, Wang J, Masui K, Paucar A, Yang H, Ohashi M, Zhu S, Wykosky J, Reed R, Nelson SF, Cloughesy TF, James CD, Rao PN, Kornblum HI, Heath JR, Cavenee WK, Furnari FB, Mischel PS, Targeted therapy resistance mediated by dynamic regulation of extrachromosomal mutant EGFR DNA. Science 343, 72–76 (2014). [PubMed: 24310612]
8. Shinojima N, Tada K, Shiraishi S, Kamiryo T, Kochi M, Nakamura H, Makino K, Saya H, Hirano H, Kuratsu J, Oka K, Ishimaru Y, Ushio Y, Prognostic value of epidermal growth factor receptor in patients with glioblastoma multiforme. Cancer Res 63, 6962–6970 (2003). [PubMed: 14583498]
9. Heimberger AB, Hlatky R, Suki D, Yang D, Weinberg J, Gilbert M, Sawaya R, Aldape K, Prognostic effect of epidermal growth factor receptor and EGFRvIII in glioblastoma multiforme patients. Clin Cancer Res 11, 1462–1466 (2005). [PubMed: 15746047]
10. Kastenhuber ER, Huse JT, Berman SH, Pedraza A, Zhang J, Suehara Y, Viale A, Cavatore M, Heguy A, Szerlip N, Ladanyi M, Brennan CW, Quantitative assessment of intragenic receptor tyrosine kinase deletions in primary glioblastomas: their prevalence and molecular correlates. Acta Neuropathol 127, 747–759 (2014). [PubMed: 24292886]
11. Weller M, Felsberg J, Hartmann C, Berger H, Steinbach JP, Schramm J, Westphal M, Schackert G, Simon M, Tonn JC, Heese O, Krex D, Nikkhah G, Pietsch T, Wiestler O, Reifenberger G, von Deimling A, Loeffler M, Molecular predictors of progression-free and overall survival in patients with newly diagnosed glioblastoma: a prospective translational study of the German Glioma Network. J Clin Oncol 27, 5743–5750 (2009). [PubMed: 19805672]
12. Felsberg J, Hentschel B, Kaulich K, Gramatzki D, Zacher A, Malzkorn B, Kamp M, Sabel M, Simon M, Westphal M, Schackert G, Tonn JC, Pietsch T, von Deimling A, Loeffler M, Reifenberger G, Weller M, German Glioma N, Epidermal Growth Factor Receptor Variant III (EGFRvIII) Positivity in EGFR-Amplified Glioblastomas: Prognostic Role and Comparison between Primary and Recurrent Tumors. Clin Cancer Res 23, 6846–6855 (2017). [PubMed: 28855349]
13. van den Bent MJ, Gao Y, Kerkhof M, Kros JM, Gorlia T, van Zwieten K, Prince J, van Duinen S, Sillevis Smitt PA, Taphoorn M, French PJ, Changes in the EGFR amplification and EGFRvIII expression between paired primary and recurrent glioblastomas. Neuro Oncol 17, 935–941 (2015). [PubMed: 25691693]
14. Montano N, Cenci T, Martini M, D'Alessandris QG, Pelacchi F, Ricci-Vitiani L, Maira G, De Maria R, Larocca LM, Pallini R, Expression of EGFRvIII in glioblastoma: prognostic significance revisited. Neoplasia 13, 1113–1121 (2011). [PubMed: 22241957]
15. Patel AP, Tirosh I, Trombetta JJ, Shalek AK, Gillespie SM, Wakimoto H, Cahill DP, Nahed BV, Curry WT, Martuza RL, Louis DN, Rozenblatt-Rosen O, Suva ML, Regev A, Bernstein BE, Single-cell RNA-seq highlights intratumoral heterogeneity in primary glioblastoma. Science 344, 1396–1401 (2014). [PubMed: 24925914]
16. Meyer M, Reimand J, Lan X, Head R, Zhu X, Kushida M, Bayani J, Pressey JC, Lionel AC, Clarke ID, Cusimano M, Squire JA, Scherer SW, Bernstein M, Woodin MA, Bader GD, Dirks PB, Single cell-derived clonal analysis of human glioblastoma links functional and genomic heterogeneity. Proc Natl Acad Sci U S A 112, 851–856 (2015). [PubMed: 25561528]
17. Darmanis S, Sloan SA, Croote D, Mignardi M, Chernikova S, Samghababi P, Zhang Y, Neff N, Kowarsky M, Caneda C, Li G, Chang SD, Connolly ID, Li Y, Barres BA, Gephart MH, Quake SR, Single-Cell RNA-Seq Analysis of Infiltrating Neoplastic Cells at the Migrating Front of Human Glioblastoma. Cell Rep 21, 1399–1410 (2017). [PubMed: 29091775]
18. Francis JM, Zhang CZ, Maire CL, Jung J, Manzo VE, Adalsteinsson VA, Homer H, Haidar S, Blumenstiel B, Pedamallu CS, Ligon AH, Love JC, Meyerson M, Ligon KL, EGFR variant heterogeneity in glioblastoma resolved through single-nucleus sequencing. Cancer Discov 4, 956–971 (2014). [PubMed: 24893890]

19. Nishikawa R, Sugiyama T, Narita Y, Furnari F, Cavenee WK, Matsutani M, Immunohistochemical analysis of the mutant epidermal growth factor, δEGFR, in glioblastoma. Brain tumor pathology 21, 53–56 (2004). [PubMed: 15700833]
20. Fan QW, Cheng CK, Gustafson WC, Charron E, Zipper P, Wong RA, Chen J, Lau J, Knobbe-Thomsen C, Weller M, Jura N, Reifenberger G, Shokat KM, Weiss WA, EGFR phosphorylates tumor-derived EGFRvIII driving STAT3/5 and progression in glioblastoma. Cancer Cell 24, 438–449 (2013). [PubMed: 24135280]
21. Rutkowska A, Stoczynska-Fidelus E, Janik K, Wlodarczyk A, Rieske P, EGFR(vIII): An Oncogene with Ambiguous Role. J Oncol 2019, 1092587 (2019).
22. Gan HK, Cvrljevic AN, Johns TG, The epidermal growth factor receptor variant III (EGFRvIII): where wild things are altered. FEBS J 280, 5350–5370 (2013). [PubMed: 23777544]
23. Lemmon MA, Schlessinger J, Ferguson KM, The EGFR family: not so prototypical receptor tyrosine kinases. Cold Spring Harb Perspect Biol 6, a020768 (2014).
24. Stec W, Rosiak K, Treda C, Smolarz M, Peciak J, Pacholczyk M, Lenart A, Grzela D, Stoczynska-Fidelus E, Rieske P, Cyclic trans-phosphorylation in a homodimer as the predominant mechanism of EGFRvIII action and regulation. Oncotarget 9, 8560–8572 (2018). [PubMed: 29492217]
25. Gajadhar AS, Bogdanovic E, Munoz DM, Guha A, In situ analysis of mutant EGFRs prevalent in glioblastoma multiforme reveals aberrant dimerization, activation, and differential response to anti-EGFR targeted therapy. Mol Cancer Res 10, 428–440 (2012). [PubMed: 22232519]
26. Hwang Y, Chumbalkar V, Latha K, Bogler O, Forced dimerization increases the activity of DeltaEGFR/EGFRvIII and enhances its oncogenicity. Mol Cancer Res 9, 1199–1208 (2011). [PubMed: 21775422]
27. Kancha RK, von Bubnoff N, Duyster J, Asymmetric kinase dimer formation is crucial for the activation of oncogenic EGFRvIII but not for ERBB3 phosphorylation. Cell Commun Signal 11, 39 (2013). [PubMed: 23758840]
28. Fernandes H, Cohen S, Bishayee S, Glycosylation-induced conformational modification positively regulates receptor-receptor association: a study with an aberrant epidermal growth factor receptor (EGFRvIII/DeltaEGFR) expressed in cancer cells. J Biol Chem 276, 5375–5383 (2001). [PubMed: 11087732]
29. Luwor RB, Zhu HJ, Walker F, Vitali AA, Perera RM, Burgess AW, Scott AM, Johns TG, The tumor-specific de2–7 epidermal growth factor receptor (EGFR) promotes cells survival and heterodimerizes with the wild-type EGFR. Oncogene 23, 6095–6104 (2004). [PubMed: 15221011]
30. Greenall SA, Donoghue JF, Van Sinderen M, Dubljevic V, Budiman S, Devlin M, Street I, Adams TE, Johns TG, EGFRvIII-mediated transactivation of receptor tyrosine kinases in glioma: mechanism and therapeutic implications. Oncogene 34, 5277–5287 (2015). [PubMed: 25659577]
31. Ymer SI, Greenall SA, Cvrljevic A, Cao DX, Donoghue JF, Epa VC, Scott AM, Adams TE, Johns TG, Glioma Specific Extracellular Missense Mutations in the First Cysteine Rich Region of Epidermal Growth Factor Receptor (EGFR) Initiate Ligand Independent Activation. Cancers (Basel) 3, 2032–2049 (2011). [PubMed: 24212795]
32. Paul MD, Hristova K, The RTK Interactome: Overview and Perspective on RTK Heterointeractions. Chem Rev 119, 5881–5921 (2019). [PubMed: 30589534]
33. Chakravarty D, Pedraza AM, Cotari J, Liu AH, Punko D, Kokroo A, Huse JT, Altan-Bonnet G, Brennan CW, EGFR and PDGFRA co-expression and heterodimerization in glioblastoma tumor sphere lines. Sci Rep 7, 9043 (2017). [PubMed: 28831081]
34. Garnett J, Chumbalkar V, Vaillant B, Gururaj AE, Hill KS, Latha K, Yao J, Priebe W, Colman H, Elferink LA, Bogler O, Regulation of HGF expression by DeltaEGFR-mediated c-Met activation in glioblastoma cells. Neoplasia 15, 73–84 (2013). [PubMed: 23359207]
35. Szerlip NJ, Pedraza A, Chakravarty D, Azim M, McGuire J, Fang Y, Ozawa T, Holland EC, Huse JT, Jhanwar S, Leversha MA, Mikkelsen T, Brennan CW, Intratumoral heterogeneity of receptor tyrosine kinases EGFR and PDGFRA amplification in glioblastoma defines subpopulations with distinct growth factor response. Proc Natl Acad Sci U S A 109, 3041–3046 (2012). [PubMed: 22323597]
36. Chen PH, Chen X, He X, Platelet-derived growth factors and their receptors: structural and functional perspectives. Biochim Biophys Acta 1834, 2176–2186 (2013). [PubMed: 23137658]

37. Jun HJ, Appleman VA, Wu HJ, Rose CM, Pineda JJ, Yeo AT, Delcuze B, Lee C, Gyuris A, Zhu H, Woolfenden S, Bronisz A, Nakano I, Chiocca EA, Bronson RT, Ligon KL, Sarkaria JN, Gygi SP, Michor F, Mitchison TJ, Charest A, A PDGFRalpha-driven mouse model of glioblastoma reveals a stathmin1-mediated mechanism of sensitivity to vinblastine. Nat Commun 9, 3116 (2018). [PubMed: 30082792]
38. Zhou S, Appleman VA, Rose CM, Jun HJ, Yang J, Zhou Y, Bronson RT, Gygi SP, Charest A, Chronic platelet-derived growth factor receptor signaling exerts control over initiation of protein translation in glioma. Life Sci Alliance 1, e201800029 (2018).
39. Roskoski R Jr., Small molecule inhibitors targeting the EGFR/ErbB family of protein-tyrosine kinases in human cancers. Pharmacol Res 139, 395–411 (2019). [PubMed: 30500458]
40. Reardon DA, Wen PY, Mellinghoff IK, Targeted molecular therapies against epidermal growth factor receptor: past experiences and challenges. Neuro Oncol 16 **Suppl** 8, viii7–13 (2014).**Suppl**
41. Sarkaria JN, Yang L, Grogan PT, Kitange GJ, Carlson BL, Schroeder MA, Galanis E, Giannini C, Wu W, Dinca EB, James CD, Identification of molecular characteristics correlated with glioblastoma sensitivity to EGFR kinase inhibition through use of an intracranial xenograft test panel. Mol Cancer Ther 6, 1167–1174 (2007). [PubMed: 17363510]
42. Sarkaria JN, Carlson BL, Schroeder MA, Grogan P, Brown PD, Giannini C, Ballman KV, Kitange GJ, Guha A, Pandita A, James CD, Use of an orthotopic xenograft model for assessing the effect of epidermal growth factor receptor amplification on glioblastoma radiation response. Clin Cancer Res 12, 2264–2271 (2006). [PubMed: 16609043]
43. Vaubel RA, Tian S, Remonde D, Schroeder MA, Mladek AC, Kitange GJ, Caron A, Kollmeyer TM, Grove R, Peng S, Carlson BL, Ma DJ, Sarkar G, Evers L, Decker PA, Yan H, Dhruv HD, Berens ME, Wang Q, Marin BM, Klee EW, Califano A, LaChance DH, Eckel-Passow JE, Verhaak RG, Sulman EP, Burns TC, Meyer FB, O'Neill BP, Tran NL, Giannini C, Jenkins RB, Parney IF, Sarkaria JN, Genomic and Phenotypic Characterization of a Broad Panel of Patient-Derived Xenografts Reflects the Diversity of Glioblastoma. Clin Cancer Res 26, 1094–1104 (2020). [PubMed: 31852831]
44. Davis MI, Hunt JP, Herrgard S, Ciceri P, Wodicka LM, Pallares G, Hocker M, Treiber DK, Zarrinkar PP, Comprehensive analysis of kinase inhibitor selectivity. Nat Biotechnol 29, 1046–1051 (2011). [PubMed: 22037378]
45. Folkes AJ, Ahmadi K, Alderton WK, Alix S, Baker SJ, Box G, Chuckowree IS, Clarke PA, Depledge P, Eccles SA, Friedman LS, Hayes A, Hancox TC, Kugendradas A, Lensun L, Moore P, Olivero AG, Pang J, Patel S, Pergl-Wilson GH, Raynaud FI, Robson A, Saghir N, Salphati L, Sohal S, Ultsch MH, Valenti M, Wallweber HJ, Wan NC, Wiesmann C, Workman P, Zhyvoloup A, Zvelebil MJ, Shuttleworth SJ, The identification of 2-(1H-indazol-4-yl)-6-(4-methanesulfonyl-piperazin-1-ylmethyl)-4-morpholin-4-yl-t hieno[3,2-d]pyrimidine (GDC-0941) as a potent, selective, orally bioavailable inhibitor of class I PI3 kinase for the treatment of cancer. J Med Chem 51, 5522–5532 (2008). [PubMed: 18754654]
46. Brown AP, Carlson TC, Loi CM, Graziano MJ, Pharmacodynamic and toxicokinetic evaluation of the novel MEK inhibitor, PD0325901, in the rat following oral and intravenous administration. Cancer Chemother Pharmacol 59, 671–679 (2007). [PubMed: 16944149]
47. Roskoski R Jr, The role of small molecule platelet-derived growth factor receptor (PDGFR) inhibitors in the treatment of neoplastic disorders. Pharmacological research 129, 65–83 (2018). [PubMed: 29408302]
48. Zhu H, Acquaviva J, Ramachandran P, Boskovitz A, Woolfenden S, Pfannl R, Bronson RT, Chen JW, Weissleder R, Housman DE, Charest A, Oncogenic EGFR signaling cooperates with loss of tumor suppressor gene functions in gliomagenesis. Proc Natl Acad Sci U S A 106, 2712–2716 (2009). [PubMed: 19196966]
49. Stommel JM, Kimmelman AC, Ying H, Nabioullin R, Ponugoti AH, Wiedemeyer R, Stegh AH, Bradner JE, Ligon KL, Brennan C, Chin L, DePinho RA, Coactivation of receptor tyrosine kinases affects the response of tumor cells to targeted therapies. Science 318, 287–290 (2007). [PubMed: 17872411]
50. McNeill RS, Canoutas DA, Stuhlmiller TJ, Dhruv HD, Irvin DM, Bash RE, Angus SP, Herring LE, Simon JM, Skinner KR, Limas JC, Chen X, Schmid RS, Siegel MB, Van Swearingen AED, Hadler MJ, Sulman EP, Sarkaria JN, Anders CK, Graves LM, Berens ME, Johnson GL, Miller

CR, Combination therapy with potent PI3K and MAPK inhibitors overcomes adaptive kinome resistance to single agents in preclinical models of glioblastoma. Neuro Oncol 19, 1469–1480 (2017). [PubMed: 28379424]

51. Schram AM, Gandhi L, Mita MM, Damstrup L, Campana F, Hidalgo M, Grande E, Hyman DM, Heist RS, A phase Ib dose-escalation and expansion study of the oral MEK inhibitor pimasertib and PI3K/MTOR inhibitor voxtalisib in patients with advanced solid tumours. Br J Cancer 119, 1471–1476 (2018). [PubMed: 30425349]
52. Wainberg ZA, Alsina M, Soares HP, Brana I, Britten CD, Del Conte G, Ezeh P, Houk B, Kern KA, Leong S, Pathan N, Pierce KJ, Siu LL, Vermette J, Tabernero J, A Multi-Arm Phase I Study of the PI3K/mTOR Inhibitors PF-04691502 and Gedatolisib (PF-05212384) plus Irinotecan or the MEK Inhibitor PD-0325901 in Advanced Cancer. Target Oncol 12, 775–785 (2017). [PubMed: 29067643]
53. Grilley-Olson JE, Bedard PL, Fasolo A, Cornfeld M, Cartee L, Razak AR, Stayner LA, Wu Y, Greenwood R, Singh R, Lee CB, Bendell J, Burris HA, Del Conte G, Sessa C, Infante JR, A phase Ib dose-escalation study of the MEK inhibitor trametinib in combination with the PI3K/mTOR inhibitor GSK2126458 in patients with advanced solid tumors. Invest New Drugs 34, 740–749 (2016). [PubMed: 27450049]
54. Bedard PL, Tabernero J, Janku F, Wainberg ZA, Paz-Ares L, Vansteenkiste J, Van Cutsem E, Perez-Garcia J, Stathis A, Britten CD, Le N, Carter K, Demanse D, Csonka D, Peters M, Zubel A, Nauwelaerts H, Sessa C, A phase Ib dose-escalation study of the oral pan-PI3K inhibitor buparlisib (BKM120) in combination with the oral MEK1/2 inhibitor trametinib (GSK1120212) in patients with selected advanced solid tumors. Clin Cancer Res 21, 730–738 (2015). [PubMed: 25500057]
55. Tolcher AW, Patnaik A, Papadopoulos KP, Rasco DW, Becerra CR, Allred AJ, Orford K, Aktan G, Ferron-Brady G, Ibrahim N, Gauvin J, Motwani M, Cornfeld M, Phase I study of the MEK inhibitor trametinib in combination with the AKT inhibitor afuresertib in patients with solid tumors and multiple myeloma. Cancer Chemother Pharmacol 75, 183–189 (2015). [PubMed: 25417902]
56. Bachoo RM, Maher EA, Ligon KL, Sharpless NE, Chan SS, You MJ, Tang Y, DeFrances J, Stover E, Weissleder R, Rowitch DH, Louis DN, DePinho RA, Epidermal growth factor receptor and Ink4a/Arf: convergent mechanisms governing terminal differentiation and transformation along the neural stem cell to astrocyte axis. Cancer Cell 1, 269–277 (2002). [PubMed: 12086863]
57. Xing Y, Wang R, Li C, Minoo P, PTEN regulates lung endodermal morphogenesis through MEK/ERK pathway. Dev Biol 408, 56–65 (2015). [PubMed: 26460096]
58. Gu J, Tamura M, Yamada KM, Tumor suppressor PTEN inhibits integrin- and growth factor-mediated mitogen-activated protein (MAP) kinase signaling pathways. J Cell Biol 143, 1375–1383 (1998). [PubMed: 9832564]
59. Ebbesen SH, Scaltriti M, Bialucha CU, Morse N, Kastenhuber ER, Wen HY, Dow LE, Baselga J, Lowe SW, Pten loss promotes MAPK pathway dependency in HER2/neu breast carcinomas. Proc Natl Acad Sci U S A 113, 3030–3035 (2016). [PubMed: 26929372]
60. Weng LP, Smith WM, Brown JL, Eng C, PTEN inhibits insulin-stimulated MEK/MAPK activation and cell growth by blocking IRS-1 phosphorylation and IRS-1/Grb-2/Sos complex formation in a breast cancer model. Hum Mol Genet 10, 605–616 (2001). [PubMed: 11230180]
61. Wee S, Jagani Z, Xiang KX, Loo A, Dorsch M, Yao YM, Sellers WR, Lengauer C, Stegmeier F, PI3K pathway activation mediates resistance to MEK inhibitors in KRAS mutant cancers. Cancer Res 69, 4286–4293 (2009). [PubMed: 19401449]
62. Weng LP, Brown JL, Baker KM, Ostrowski MC, Eng C, PTEN blocks insulin-mediated ETS-2 phosphorylation through MAP kinase, independently of the phosphoinositide 3-kinase pathway. Hum Mol Genet 11, 1687–1696 (2002). [PubMed: 12095911]
63. Snuderl M, Fazlollahi L, Le LP, Nitta M, Zhelyazkova BH, Davidson CJ, Akhavanfard S, Cahill DP, Aldape KD, Betensky RA, Louis DN, Iafrate AJ, Mosaic amplification of multiple receptor tyrosine kinase genes in glioblastoma. Cancer Cell 20, 810–817 (2011). [PubMed: 22137795]
64. Serrano M, Lee H, Chin L, Cordon-Cardo C, Beach D, DePinho RA, Role of the INK4a locus in tumor suppression and cell mortality. Cell 85, 27–37 (1996). [PubMed: 8620534]

65. Lesche R, Groszer M, Gao J, Wang Y, Messing A, Sun H, Liu X, Wu H, Cre/loxP-mediated inactivation of the murine Pten tumor suppressor gene. Genesis 32, 148–149 (2002). [PubMed: 11857804]

66. Shin KJ, Wall EA, Zavzavadjian JR, Santat LA, Liu J, Hwang JI, Rebres R, Roach T, Seaman W, Simon MI, Fraser ID, A single lentiviral vector platform for microRNA-based conditional RNA interference and coordinated transgene expression. Proc Natl Acad Sci U S A 103, 13759–13764 (2006). [PubMed: 16945906]

67. Madisen L, Zwingman TA, Sunkin SM, Oh SW, Zariwala HA, Gu H, Ng LL, Palmiter RD, Hawrylycz MJ, Jones AR, Lein ES, Zeng H, A robust and high-throughput Cre reporting and characterization system for the whole mouse brain. Nat Neurosci 13, 133–140 (2010). [PubMed: 20023653]

68. Jun HJ, Bronson RT, Charest A, Inhibition of EGFR induces a c-MET-driven stem cell population in glioblastoma. Stem Cells 32, 338–348 (2014). [PubMed: 24115218]

69. Jun HJ, Acquaviva J, Chi D, Lessard J, Zhu H, Woolfenden S, Bronson RT, Pfannl R, White F, Housman DE, Iyer L, Whittaker CA, Boskovitz A, Raval A, Charest A, Acquired MET expression confers resistance to EGFR inhibition in a mouse model of glioblastoma multiforme. Oncogene 31, 3039–3050 (2012). [PubMed: 22020333]

70. Acquaviva J, Jun HJ, Lessard J, Ruiz R, Zhu H, Donovan M, Woolfenden S, Boskovitz A, Raval A, Bronson RT, Pfannl R, Whittaker CA, Housman DE, Charest A, Chronic activation of wild-type epidermal growth factor receptor and loss of Cdkn2a cause mouse glioblastoma formation. Cancer Res 71, 7198–7206 (2011). [PubMed: 21987724]

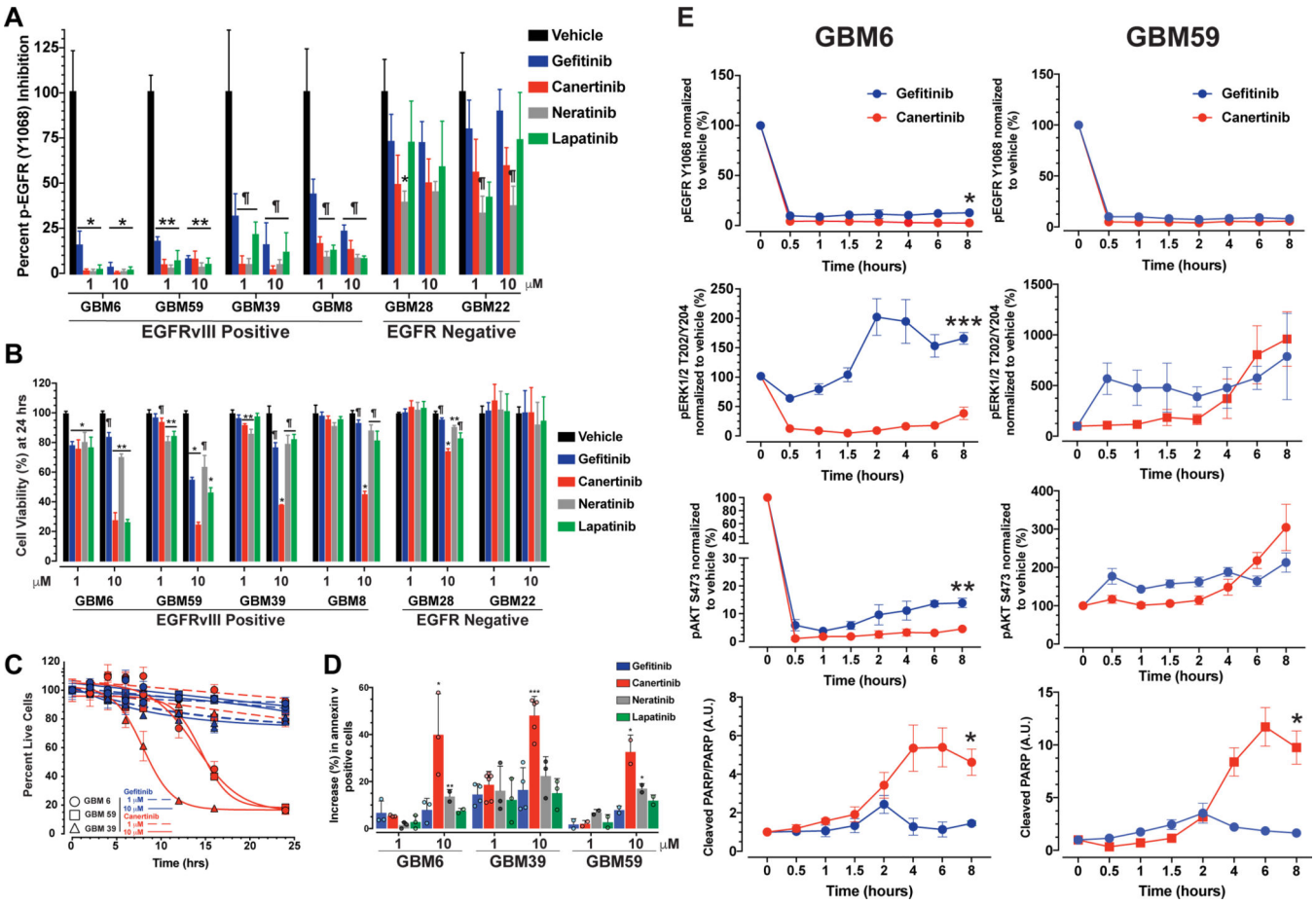

Figure 1. Canertinib treatments induce apoptosis in EGFRvIII GBM PDXs.

A panel of EGFRvIII positive GBM PDX lines, GBM6, GBM59, GBM39, GBM8, and EGFR negative GBM28 and GBM22 were treated with either 1 μM or 10 μM Gefitinib, Canertinib, Neratinib and Lapatinib for 6 hours. **A)** Graphical representation of EGFR kinase inhibition assessed by quantitative western blot analysis of the autophosphorylation tyrosine1068 in biological replicates (n=3) post inhibitor treatments compared to vehicle (DMSO) treatment. Plotted are averages, analyzed for statistical significance using Student's t test, two tailed. Error bars S.D., * p<0.01, ¶<0.05, ** p<0.005. **B)** Graphical representation of cell viability assessed using XTT assays post inhibitor treatments and normalized to DMSO-treated controls. Plotted are averages, analyzed for statistical significance using Student's t test, two tailed. Error bars S.D., * p<0.0001, ** p<0.001. ¶<0.05. **C)** Dynamics of cell death in GBM6, GBM59 and GBM39 upon treatments with Gefitinib and Canertinib. XTT assays were performed to determine number of viable cells over a 24 hrs time course in presence of vehicle DMSO as control or 1 and 10 μM Gefitinib and Canertinib in biological replicates (n=3). Data is normalized to DMSO control and plotted as averages, error bars +/− S.D. **D)** Increase in apoptosis in cells treated with 10 μM Canertinib. GBM6, GBM39 and GBM59 cells were treated with 1 and 10 μM of the indicated EGFR inhibitors for 24 hrs in biological replicates (n=3) and cells were harvested and processed for propidium iodine and annexin V staining and flow cytometry. The percentage of annexin V positive cells are plotted relative to DMSO treated controls. Plotted are averages, analyzed for statistical

significance using Student's t test, two tailed. Error bars S.D., * $p<0.03$, ** $p<0.008$ and *** $p<0.0001$. **E)** Dynamics of EGFR kinase inhibition as measured by quantitative western blots of phospho-EGFR Y1068 and canonical EGFR signaling pathway members phospho-ERK1/2 T202/Y204 and phospho-AKT S473 in GBM6 and GBM39 treated with 10 μM of Gefitinib and Canertinib for the indicated times. Plotted are averages of percent inhibitions when compared to vehicle (DMSO) treatments in biological replicates (n=3). Error bars S.D. 8 hrs time points of Canertinib treated versus Gefitinib treated, * $p<0.02$, ** $p<0.006$ and *** $p<0.001$.

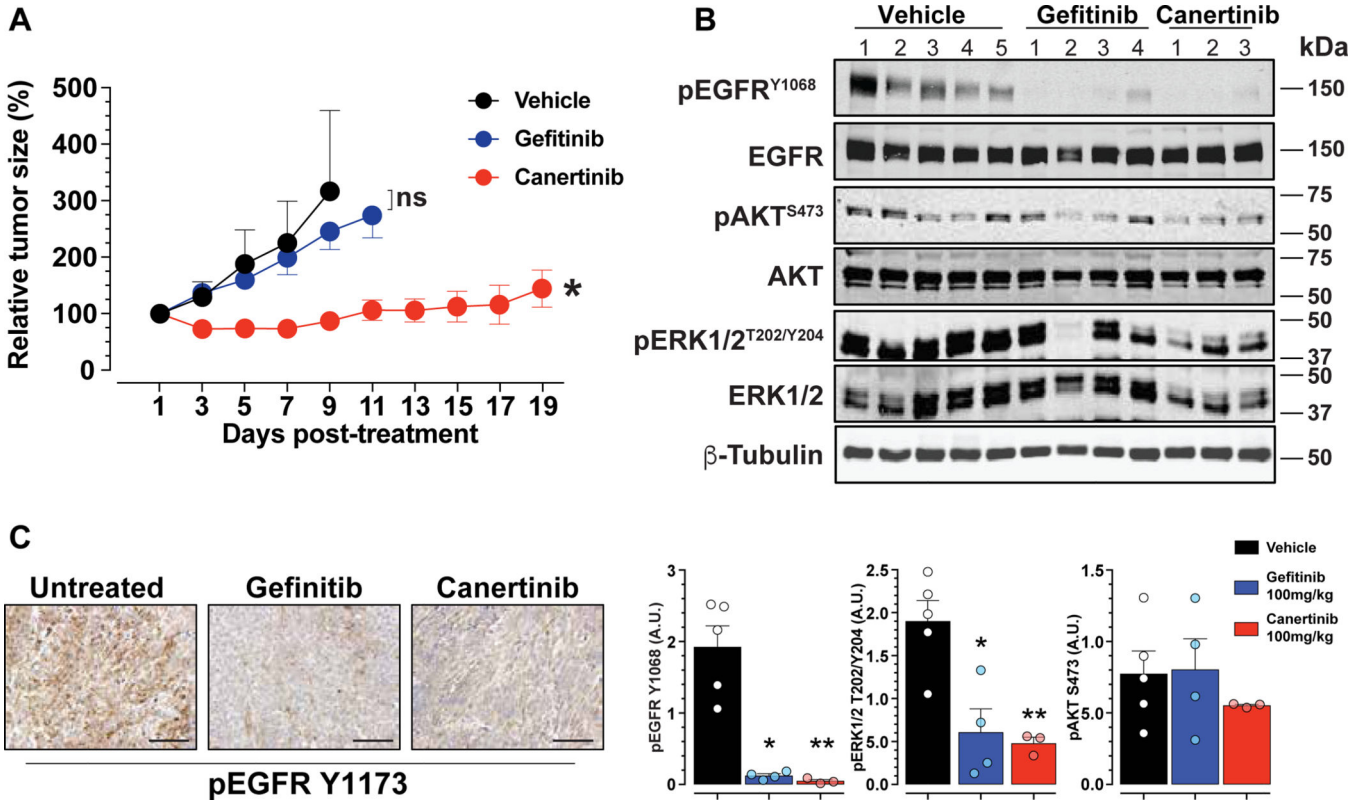

Figure 2. Anti-growth efficacy of Canertinib in vivo.

A) Tumor volumes of the GBM6 PDX line grown in subcutaneous flanks of immunocompromised $Ncr^{Nu/Nu}$ mice. Upon reaching ~100 mm^3, mice were randomized to vehicle, Gefitinib (100 mg/kg) or Canertinib (100 mg/kg) by oral gavage daily. Tumor responses are expressed as the percentage change from the baseline tumor volumes at the time of treatment initiation (~100 mm^3, Day 1). Vehicle n = 5, Gefitinib n=4, Canertinib n=3, *p<0.03 by Student t-test. **B)** Representative photomicrograph (top) and graphical representation of quantification (bottom) of western blotting of extracts from endpoint tumors (A) probed against the indicated proteins. Quantification of the western blot is achieved by calculating levels of pEGFR/EGFR/β-tubulin, pERK1/2/ERK1/2/β-tubulin and pAKT/AKT/β-tubulin. A.U.: arbitrary units. pEGFR *p=0.0011, **p=0.0032; pERK1/2 *p=0.0094, **p=0.0048 by student t-test. **C)** Representative photomicrographs of anti-phospho-EGFR Tyr1173 immunohistochemistry from tumors in (A). Scale bar=100 μm.

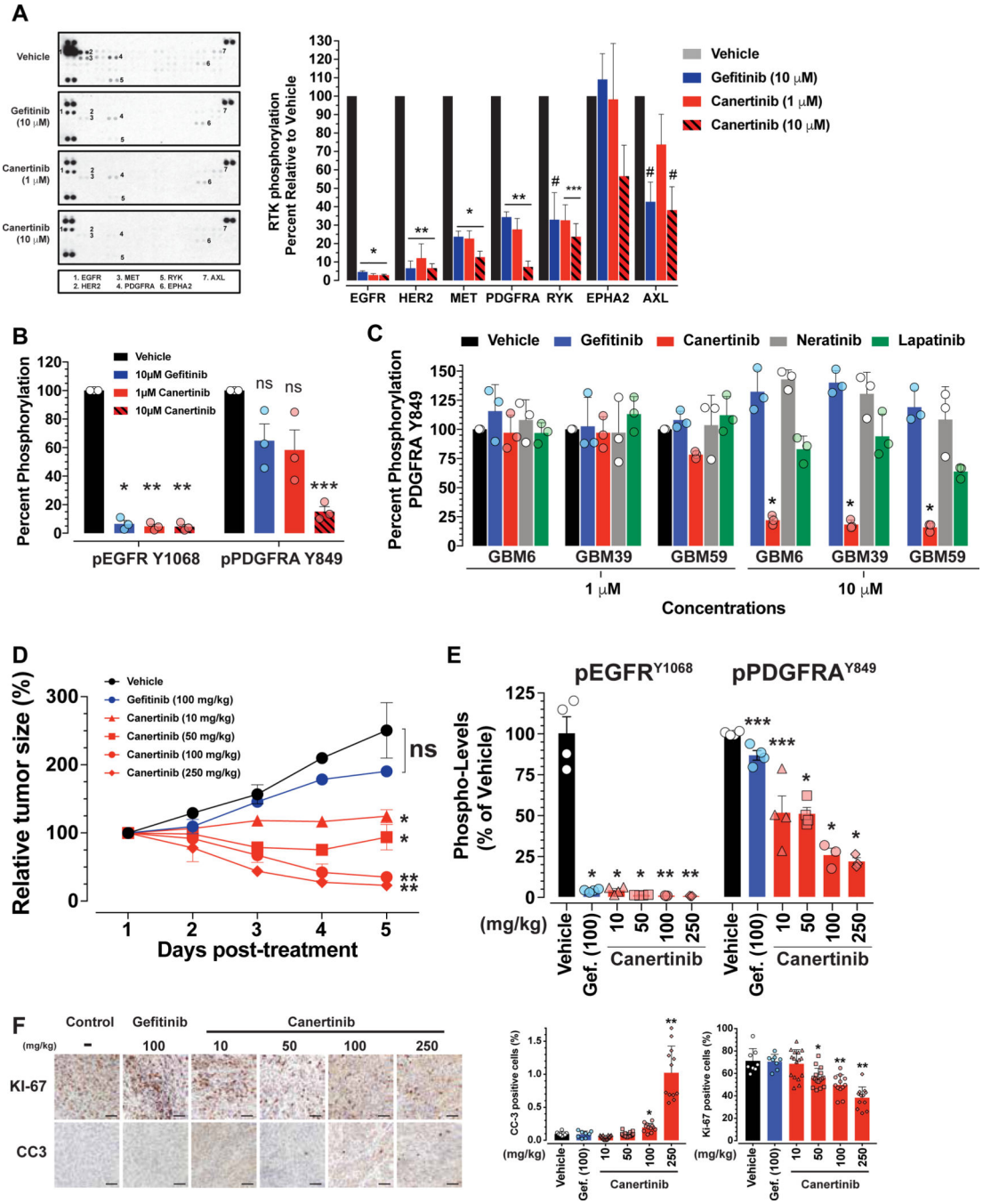

Figure 3. Canertinib treatment decreases the activity of PDGFRA and demonstrates dose-dependent anti-tumor activity.

A) Representative image of a phospho-RTK array of GBM6 cells (left). Cells were treated with vehicle (DMSO), 1 μM Canertinib, 10 μM Gefitinib or Canertinib for 4 hrs and lysates were used on the reverse phase protein arrays. Quantification of triplicate RTK arrays (right). Dots were quantified using the ImageJ software and percent reduction in RTK phosphorylation compared to vehicle treated was calculated. Statistical analysis, mean ± S.D. n=3, student t-test, #p<0.01, *p<0.0001, **p<0.0005, ***p<0.001. **B)** Validation of

levels of phosphorylated EGFR and PDGFRA by western blotting. Graphical representation of the quantification of western blots showing the percent reduction in phospho-EGFR and phospho-PDGFRA when compared to vehicle treated. Statistical analysis, mean ± S.D., n=3 biological triplicates, student t-test, *p=0.0007, **p=0.0003, ***p=0017. **C)** High concentrations of Canertinib selectively inhibit PDGFRA in GBM6, GBM39 and GBM59. Bar graph of quantification of western blots of phospho-PDGFRA in GBM6, GBM39 and GBM59 treated with the indicated inhibitors plotted as percent reduction of treated compared to vehicle control. Statistical analysis, mean ± S.D., n=3 biological triplicates, student t-test, *p<0.0001. **D)** Canertinib dose-dependent reduction in tumor growth. Tumor volumes of the GBM6 PDX line grown in subcutaneous flanks of immunocompromised $Ncr^{Nu/Nu}$ mice. Upon reaching ~100 mm3, mice were randomized to vehicle, Gefitinib (100 mg/kg) or different doses of Canertinib (as indicated) by oral gavage daily. Tumor responses are expressed as the percentage change from the baseline tumor volumes at the time of treatment initiation (~100 mm^3, Day 1). Vehicle n = 4, Gefitinib n=4, Canertinib n=4 for 10 and 50 mg/kg and n=3 for 100 and 250 mg/kg, *p<0.02, **p<0.007 by Student t-test. **E)** Graphical representation of the quantification of western blots for all tumors probed for phospho-EGFR, total EGFR, phospho-PDGFRA, total PDGFRA and β-tubulin. Data is represented as percentage of levels of phospho-EGFR tyr1068/EGFR/β-tubulin and phospho-PDGFRA/PDGFRA/β-tubulin. Vehicle n=4, Gefitinib n=4, Canertinib n=4 for 10 and 50 mg/kg and n=3 for 100 and 250 mg/kg, *p<0.003, **p<0.009, ***p<0.02 by Student t-test. **F)** Decreases in cell proliferation and increases in apoptotic cell numbers upon Canertinib treatment in a dose-dependent manner. Representative photomicrographs (left) of IHC staining with the proliferative marker Ki-67 and the apoptotic marker cleaved caspase-3 (CC3) from control untreated GBM6 tumors or treated with the indicated inhibitors. Scale bar=50 μm. Graphical representation (right) of the quantification of the CC3 and Ki-67 IHC. CC3 IHC * p=0.0007, ** p<0.0001, Ki-67 IHC * p=0.001, ** p=0.0001

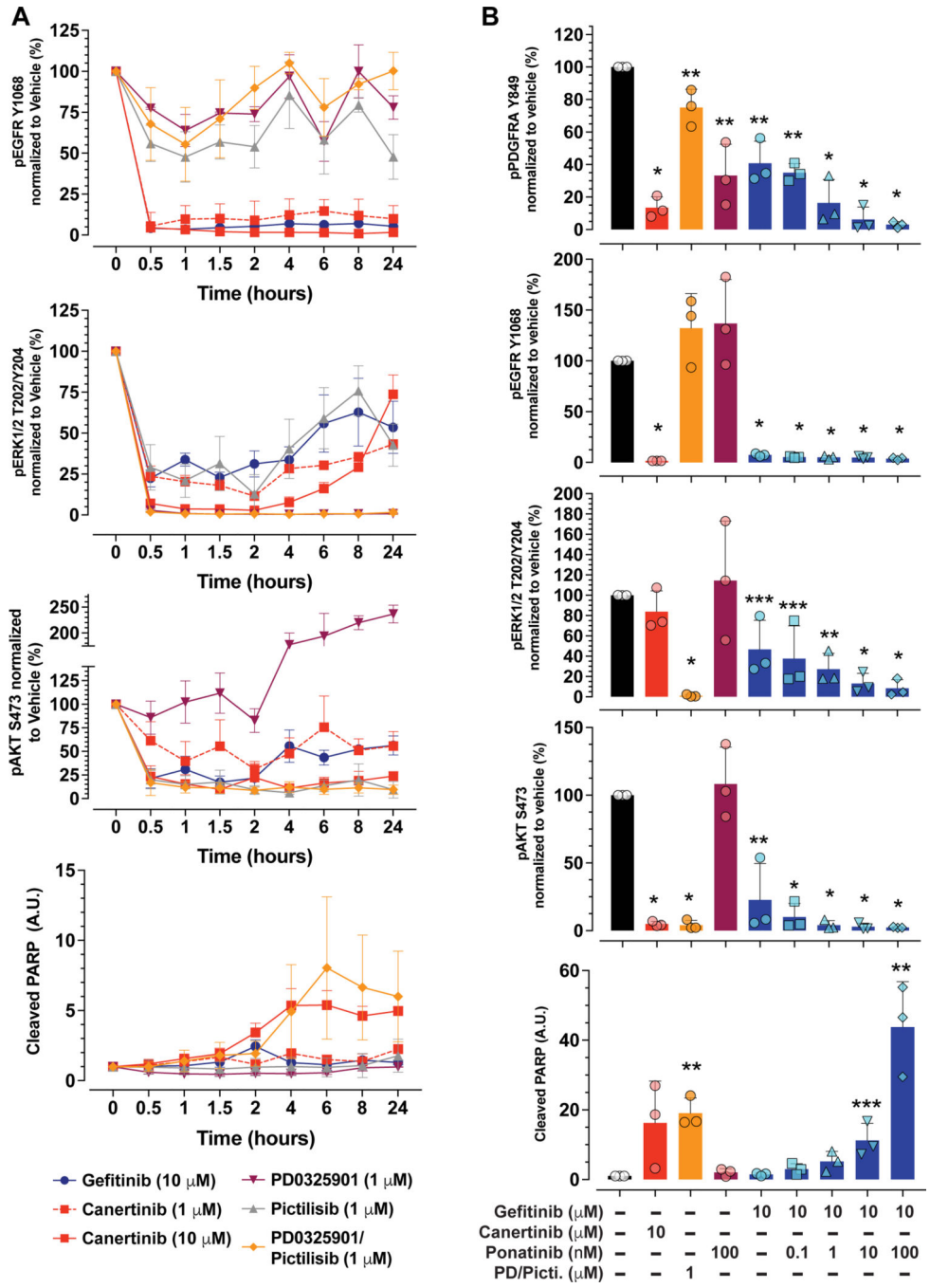

Figure 4. Simultaneous inhibition of MEK1/2 and PI3K signaling is necessary to trigger apoptosis in GBM6 PDX cells.

A) Graphical representation of quantification of western blot analyses of GBM6 cells treated with the indicated inhibitors over time and probed for the phosphoprotein targets EGFR Y1068, ERK1/2 T202/Y204 and AKT S473, the ladder two serving as surrogate of MEK1/2 and PI3K activity respectively, and the apoptosis marker cleaved PARP. The data is represented as mean ± S.D., n=3. **B)** Graphical representation of quantification of western blot analyses of GBM6 cells treated for 24 hr with dual inhibition of EGFR (10 μM

Gefitinib) and PDGFRA (Ponatinib). Statistical analysis, mean ± S.D., n=3, student t-test, *p<0.0001, **p<0.005, ***p<0.04.

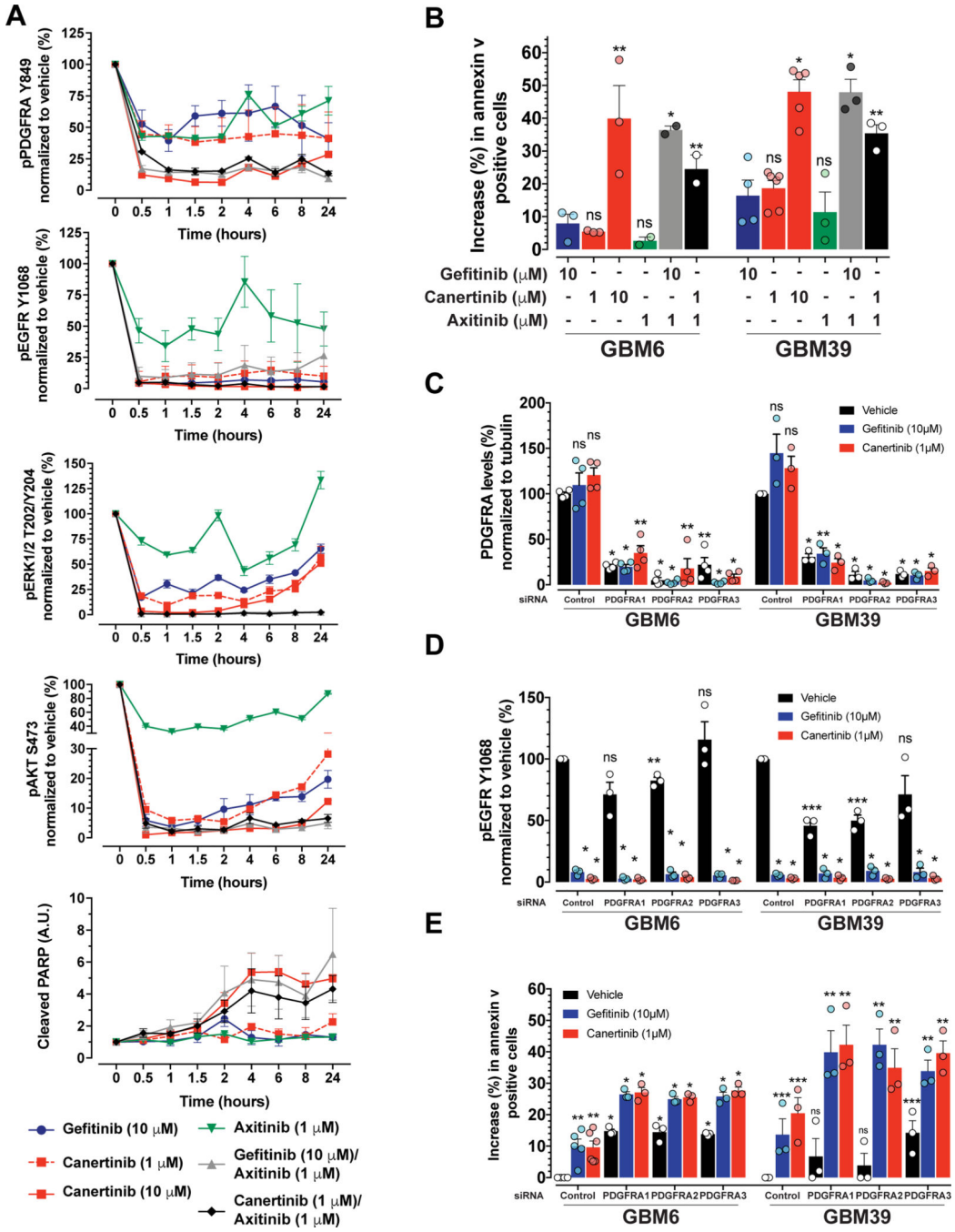

Figure 5. Inhibition of PDGFRA sensitizes GBM PDX cells to EGFR inhibition.

A) Graphical representation of quantification of western blot analyses of GBM6 cells treated with the indicated inhibitors over time and probed for the phosphoprotein targets EGFR Y1068, PDGFRA Y849, ERK1/2 T202/Y204 and AKT S473, and for the apoptosis marker cleaved PARP. The data is represented as mean ± S.D., n=3. **B)** Graphical representation of the increase in annexin V positive cells by flow cytometry from GBM6 and GBM39 cells treated with the indicated inhibitors for 24 hrs. The data is represented as mean ± S.D., n=3, student t-test, *p<0.005, **p<0.05. **C,D)** RNAi knock down of PDGFRA in

GBM6 and GBM39. Graphical representations of the quantitation of the western blot of GBM6 and GBM39 cells transiently transfected with siRNAs designed against PDGFRA and treated with the indicated inhibitors and assayed for PDGFRA protein levels (C), and phospho-EGFR (D). The data is represented as mean ± S.D., n>= 3, student t-test, PDGFRA levels (C) *p<0.0001, **p<0.0005, pEGFR Y1068 levels (D), *p<0.0001, **p=0.02 and ***p<0.0005. E) Graphical representation of flow cytometry analysis of GBM6 and GBM39 cells transiently transfected with siRNAs designed against PDGFRA and treated with the indicated inhibitors analyzed for annexin v. Data is represented as percent increase in positive cells over controls. *p<0.0001, **p<0.005 and ***p<0.05.

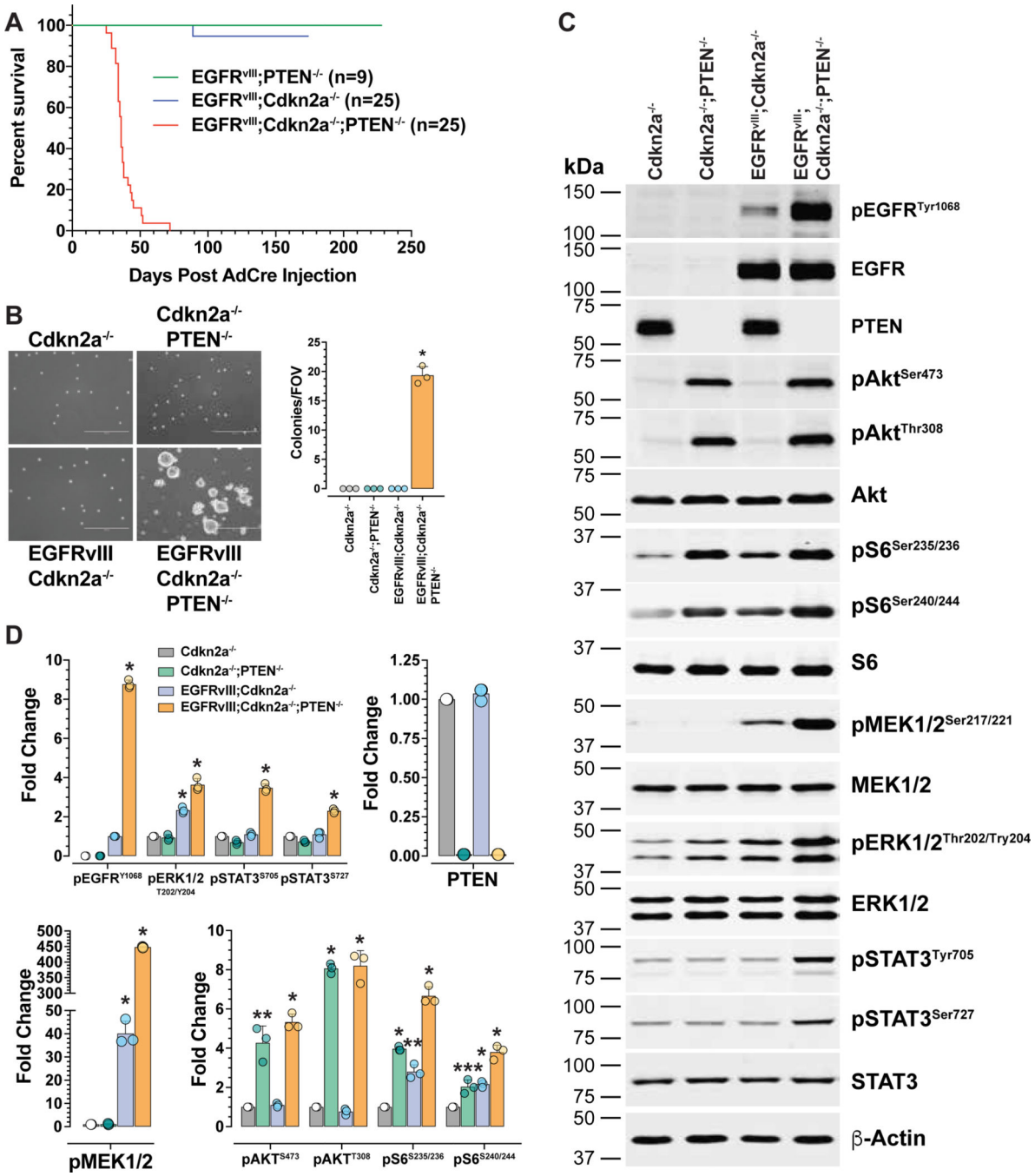

Figure 6. EGFRvIII expression requires co-signaling for cellular transformation in vitro and GBM tumor formation in vivo.

A) Kaplan-Meier survival of cohorts of mice with the indicated genotypes after intracranial stereotactic injections of Adenovirus Cre. **B)** Representative micrographs and quantification of growth in soft agar of astrocytes of the indicated genotypes. Scale bar= 400 μm. **C)** Representative quantitative western blot with lysates from the indicated cells and blotted for the indicated phospho-proteins. **D)** Graphical representation of the quantitation of the

western blots in (C). Statistical analysis for (B) and (D), mean ± S.D., n=3, student t-test, *p<0.0002, **p<0.003, ***p=0.007.

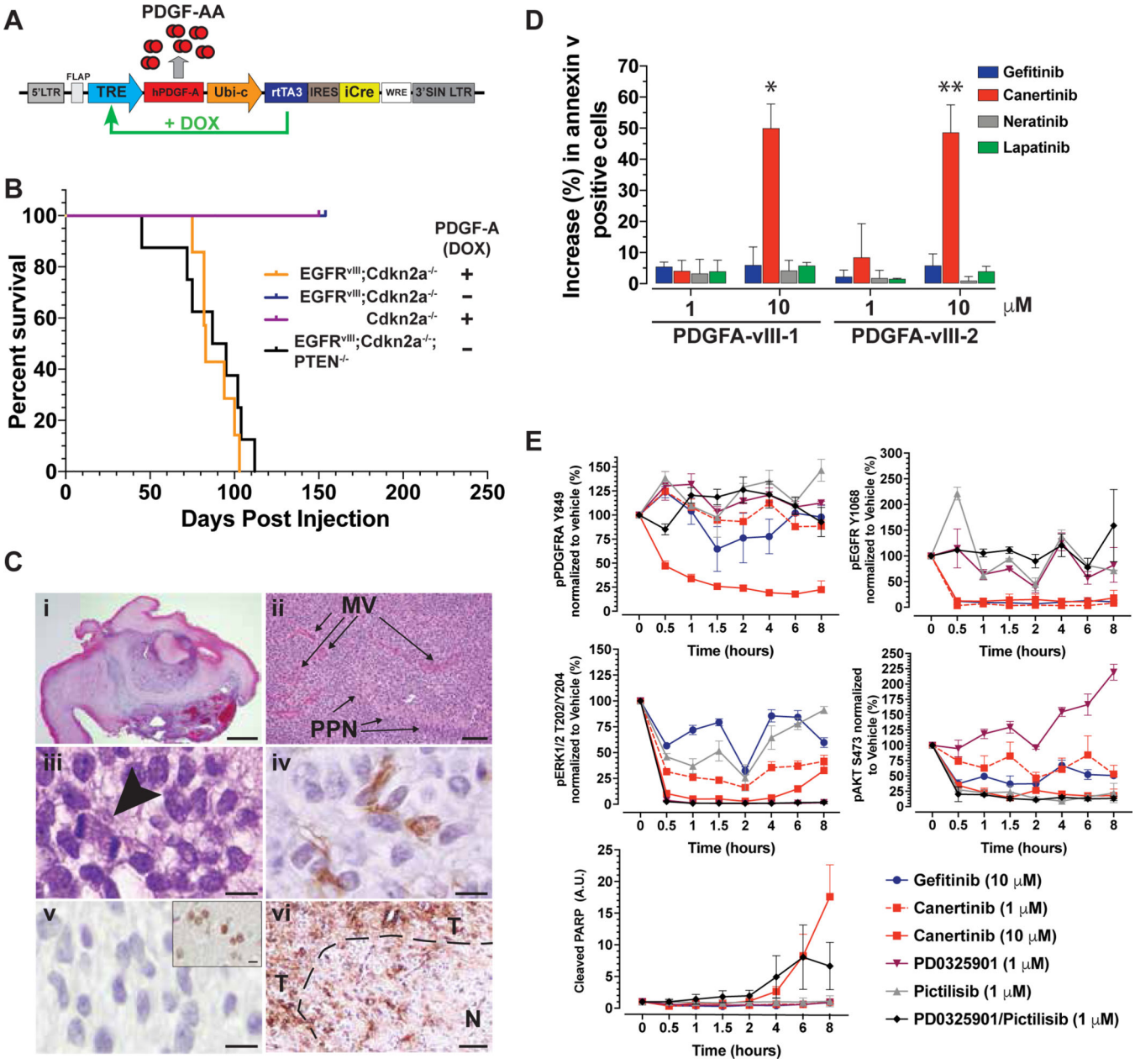

Figure 7. PDGFRA activation cooperates with EGFRvIII to initiate GBM tumorigenesis in vivo.

A) Schematic representation of the lentivirus designed for dual expression of Cre and PDGF-A ligand cDNA in a doxycycline (DOX) inducible manner. **B)** Survival (Kaplan-Meier) analysis of conditional PDGFA-EGFRvIII;Cdkn2a$^{-/-}$ mice. Cohorts of mice with the indicated genotype were injected with pSLIK-PDGFA-Cre virus and fed with or without a DOX-based diet and monitored for survival over time. **C)** PDGFA-EGFRvIII;Cdkn2a$^{-/-}$ tumors have features of GBM. Representative photomicrographs of FFPE tumor sections stained with H&E (scale bars i=1mm, ii=100 μm, iii=10 μm, MV, microvascular proliferation; PPN, pseudopalisading necrosis) and IHC for GFAP (iv, scale bar= 10 μm) and NeuN (v, scale bar=10 μm, inset: contralateral normal brain, scale bar=10 μm) and EGFR (vi, scale bar=50 μm, T, tumor; N, normal brain). **D)** Primary cell

cultures derived from individual PDGFA-EGFRvIII;Cdkn2a$^{-/-}$ GBMs were treated with the indicated EGFR TKIs for 24 h and assessed for apoptosis by PI/Annexin V staining and flow cytometry. Data is represented as percent increase in Annexin V staining from vehicle treated. Statistical analysis, mean ± S.D., n=3, student t-test, *p=0.0012, **p=0.0007. **E)** Graphical representation of quantification of western blot analysis of lysate from PDGFA-EGFRvIII;Cdkn2a$^{-/-}$ GBM cultures treated with the indicated inhibitors over time.